In Vitro Cell. Dev. Biol.—Animal 35:441–448, September 1999

1071-2690/99 $05.00+0.00

GEOMETRIC CONTROL OF SWITCHING BETWEEN GROWTH, APOPTOSIS, AND DIFFERENTIATION DURING ANGIOGENESIS USING MICROPATTERNED SUBSTRATES

LAURA E. DIKE, CHRISTOPHER S. CHEN, MILAN MRKSICH, JOE TIEN, GEORGE M. WHITESIDES, AND DONALD E. INGBER[1]

Department of Pathology, Boston University School of Medicine, Boston, Massachusetts 02118 (L. E. D.), Departments of Surgery and Pathology, Children's Hospital and Harvard Medical School, Enders 1007, 300 Longwood Avenue, Boston, Massachusetts 02115 (C. S. C., D. E. I.), and Department of Chemistry and Chemical Biology, Harvard University, Cambridge, Massachusetts 02138 (M. M., J. T., G. M. W.)

(Received 28 January 1999; accepted 12 April 1999)

SUMMARY

Past studies using micropatterned substrates coated with adhesive islands of extracellular matrix revealed that capillary endothelial cells can be geometrically switched between growth and apoptosis. Endothelial cells cultured on single islands larger than 1500 μm^2 spread and progressed through the cell cycle, whereas cells restricted to areas less than 500 μm^2 failed to extend and underwent apoptosis. The present study addressed whether island geometries that constrained cell spreading to intermediate degrees, neither supporting cell growth nor inducing apoptosis, cause cells to differentiate. Endothelial cells cultured on substrates micropatterned with 10-μm-wide lines of fibronectin formed extensive cell–cell contacts and spread to approximately 1000 μm^2. Within 72 h, cells shut off both growth and apoptosis programs and underwent differentiation, resulting in the formation of capillary tube-like structures containing a central lumen. Accumulation of extracellular matrix tendrils containing fibronectin and laminin beneath cells and reorganization of platelet endothelial cell adhesion molecule-positive cell–cell junctions along the lengths of the tubes preceded the formation of these structures. Cells cultured on wider (30-μm) lines also formed cell–cell contacts and aligned their actin cytoskeleton, but these cells spread to larger areas (2200 μm^2), proliferated, and did not form tubes. Use of micropatterned substrates revealed that altering the geometry of cell spreading can switch endothelial cells among the three major genetic programs that govern angiogenesis—growth, apoptosis and differentiation. The system presented here provides a well-defined adhesive environment in which to further investigate the steps involved in angiogenesis.

Key words: capillary tubes; morphogenesis; cell adhesion; extracellular matrix; microfabrication.

INTRODUCTION

Angiogenesis, the formation of new capillary blood vessels, plays a critical role in tissue growth and homeostasis, as well as in the pathogenesis of many diseases such as cancer, diabetic retinopathy, and rheumatoid arthritis (10). The recent findings that inhibition of angiogenesis can prevent the growth of tumors in mice (17,26,27) and possibly in humans (20), without producing systemic side effects, has focused enormous attention on the mechanism of capillary development. Despite its clinical importance, however, the mechanisms that regulate angiogenesis remain unclear.

While angiogenesis is initiated through the action of soluble mitogens, such as fibroblast growth factor (FGF) (5,11), the response of capillary endothelial (CE) cells to these factors—whether to grow, differentiate, or die—is dictated within the tissue microenvironment (4,15) by local binding interactions between cells and extracellular matrix (ECM) molecules (15,16). The mechanism by which ECM exerts this control remains controversial. Previous in vitro studies have established that varying the density of ECM molecules such as fibronectin (FN) immobilized on dishes can switch CE cells between growth and differentiation (capillary tube formation) in the presence of soluble mitogens. This switch appears to be regulated through the changes in cell spreading that directly result from varying the density of immobilized ECM molecules (13,16). In this approach, however, changes in ECM density also influence the efficiency of binding and activation of cell surface integrin receptors which can trigger intracellular signaling pathways (23,28,31,32) and alter gene expression (9) required for growth. Thus, it is unclear whether the switch between cellular programs is caused by the change in cell geometry or a change in ECM-integrin receptor binding.

To determine whether a mechanical (shape-related) signaling mechanism is critical for regulating gene programs in CE cells, we used a recently developed micropatterning technique to control cell spreading independently from ECM coating density (24,25). We engineered micrometer-scale adhesive islands surrounded by nonadhesive regions; each island was coated with a high density of ECM molecule to promote optimal integrin clustering. The size and shape of the islands controlled the degree to which the cells spread (2,35). Using this method, we previously demonstrated that CE cells can be geometrically switched between apoptosis (programmed cell death) and growth. Cells adherent to FN-coated adhesive islands that restricted cell size (mean projected area <500 μm^2) underwent apop-

[1]To whom correspondence should be addressed.

tosis, whereas cells on islands that permitted spreading (mean projected area >1500 μm²) were able to enter S phase, with the highest growth rates observed in the most highly spread cells (>3000 μm²) (2). *Mechanical interactions between CE cells and ECM that alter* cell shape also may play a role in control of capillary tube formation (16). Thus, in the present study, we used this method to explore whether CE cells geometrically constrained to a moderate degree are induced to turn on a differentiation program.

Materials and Methods

Preparation of micropatterned substrates. Microcontact printing was used to fabricate substrates patterned with regions supportive of or resistant to ECM protein adsorption, as previously described (14,25,35). Briefly, patterned silicon masters were produced by photolithography (3). Poly-(dimethylsiloxane) stamps with surface topographies complementary to those of the silicon masters were created by polymerizing a silicone prepolymer (Sylgard 184, Dow Corning Corp., Midland, MI) on top of the masters. Glass coverslips (No. 2, Corning Glass Works, Corning, NY) were coated with thin *films of titanium* (1.5 nm) followed by a thin film of gold (11.5 nm) by electron beam evaporation. To pattern a gold-coated coverslip, a cotton swab was wetted with a solution of hexadecanethiol ($HS(CH_2)_{15}CH_3$) (Aldrich, Milwaukee, WI) (2 m*M* in ethanol) and swabbed across the face of an elastomeric stamp. The stamp was dried under a stream of nitrogen gas and placed on the gold-coated glass coverslip. The stamp was removed, and the coverslip was covered with a solution of the *tri(ethylene glycol)-terminated alkanethiol* $HS(CH_2)_{11}(OCH_2CH_2)_3OH$ (2 m*M* in ethanol) for 1 h and then rinsed in ethanol. Immediately prior to use, the patterned coverslips were coated with FN (Organon Teknika-Cappel, Malvern, PA) [25 μg/ml in phosphate-buffered saline (PBS)] for 1–2 h, rinsed well with PBS, and transferred to petri dishes containing 1% bovine serum albumin (BSA) in Dulbecco's modified Eagle's medium (DMEM).

Endothelial cell culture. Bovine CE cells were cultured as described previously (16). Cell monolayers were dissociated by brief exposure to trypsin-EDTA, washed, and resuspended with 1% bovine serum albumin (BSA)/DMEM. One-half volume of 1% BSA/DMEM was removed from petri dishes containing coverslips and replaced with an equal volume of medium containing 1×10^6 CE cells/100 mm dish. High density lipoprotein (HDL) and transferrin were added to a final concentration of 10 μg/ml and 5 μg/ml, respectively. The cells were allowed to adhere for 2 h, after which 75% of the medium was removed and replaced with either defined medium (DM) [10 μg HDL per, 5 μg transferrin per ml, 3 ng fibroblast growth factor (FGF) per ml, 1% BSA] or with DMEM containing 10% calf serum and FGF (0.5 ng/ml). Cultures were maintained over a period of 3–7 d and medium was replaced every 2 d. Cells were photographed with a Nikon Diaphot phase contrast microscope onto Kodak TMAX-400 film.

Immunofluorescence microscopy. Cultured cells were rinsed with PBS and were fixed either with 4% paraformaldehyde directly or after extraction with *cytoskeletal stabilizing buffer* (CSK buffer) [50 m*M* NaCl, 150 m*M* sucrose, 3 m*M* $MgCl_2$, 10 m*M* piperazine-*N*,*N*′-bis(2-ethanesulfonic acid (PIPES), pH 6.8 and 0.5% Triton X-100] that contained the proteinase inhibitors aprotinin (20 μg/ml), leupeptin (1 μg/ml), pepstatin (1 μg/ml) and 0.1 m*M*, 4-(2 Aminoethyl)-benzenesulfonyl-fluoride (AEBSF) (Boehringer Mannheim Biochemicals, Indianapolis, IN) (28). Slides were rinsed with PBS, permeabilized with immunofluorescence (IF) buffer (*0.2% Triton X-100, 0.1% BSA in PBS*), and incubated with fluorescein-labeled phalloidin (Sigma Chemical Co., St. Louis, MO) (diluted 1:1000 in IF buffer) or with primary antibodies to platelet endothelial cell adhesion molecule (PECAM) (Transduction Laboratories, Lexington, KY), fibronectin (Sigma), or laminin (Sigma). Primary antibodies were visualized with affinity-purified rhodaminated goat anti-rabbit or anti-mouse antibodies. Immunofluorescence images were photographed with a Zeiss Axiomat microscope or a Leica confocal microscope. In some confocal microscopy studies, CE cells were stained with a cytoplasmic dye, 5-chloromethylfluorescein diacetate (CMFDA; Molecular Probes) for 30 min (1 μ*M*) prior to fixation with 4% paraformaldehyde.

Apoptosis assay. Samples were stained for apoptosis-induced DNA damage by the TUNEL method (TdT-mediated dUTP nicked labeling) and for nuclear condensation and fragmentation with DAPI (4,6-diamidino-2-phenylindole) staining. Samples were fixed with 4% paraformaldehyde for 30 min, washed with 0.1% BSA in PBS, and permeabilized with 0.1% Triton X-100 in 0.1% sodium citrate buffer. Samples were incubated with terminal deoxyribonucleic acid transferase in reaction buffer containing fluoresceinated-dUTP (Boehringer Mannheim) for 1 h, washed, and incubated with DAPI (3 mg/ml). Apoptosis was quantified as the percentage of individual cells that stained positively for TUNEL or the percentage that showed evidence of nuclear condensation and fragmentation when visualized with DAPI. A minimum of 200 cells were counted in each sample. These two methods of quantifying apoptosis were statistically indistinguishable. The apoptotic index reported here used the TUNEL assay because it is more sensitive than visualization with DAPI.

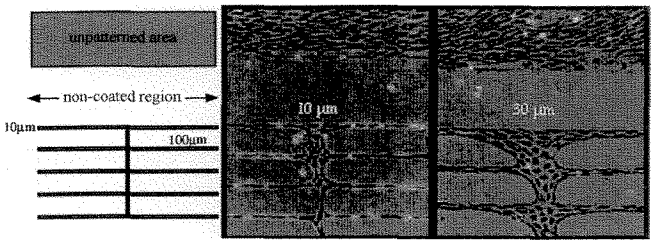

FIG. 1. Cell patterning by microcontact printing. Linear patterns consisting of multiple 10- or 30-μm-wide lines, separated by a nonadherent space of 100 μm, were formed by microcontact printing. A larger unpatterned region was included (*top of view*) as an internal control. After being coated with FN, CE cells were cultured on the patterned surface in defined medium or in medium containing 10% calf serum; cells did not attach to the uncoated barrier regions. Pattern integrity was maintained throughout the 72-h period of culture. Some cells, however, were able to extend as a monolayer over the corner portions of the nonadhesive regions. Magnification, ×100.

Determination of cell area. Image processing software (BDS Image Oncor, Rockville, MD) was used to calculate projected cell and nuclear areas from images retrieved from the microscope by a CCD camera. The projected cell area was determined from interactive tracing of cell edges drawn from phase-contrast images, as previously described (2).

DNA synthesis. CE cells were plated onto patterned substrates as described and labeled with 3 μCi [^{3}H]thymidine (1–10 Ci/mmol; Amersham Corp, IL) at 24-h intervals. Cells were rinsed with PBS, fixed with 20% methanol, and air dried. Coverslips were dipped in photographic emulsion (Kodak Corp., NY) and stored in light-tight, desiccated containers for 72 h. Coverslips were developed with D-19 developer (Kodak), fixed with Kodak fixer and rinsed with distilled water for 15 min. Cells were counterstained with Giemsa stain, and 200–300 nuclei were counted for each point.

Results

Patterned adhesive islands of defined size, shape, and position on *the micrometer scale were created by microcontact printing of self-*assembled monolayers of alkanethiols, as previously described (29). The adhesive regions were coated with a high density of the ECM component, FN, that promotes integrin receptor binding and clustering. The alkanethiols in the nonadhesive boundary regions that separate the adhesive islands were terminated in a tri(ethylene)glycol which prevents ECM adsorption and hence prohibits cell adhesion (35). A saturating amount of the growth factor, FGF, was included in the medium such that the only variable in the system was the geometry of the adhesive area onto which the cells attached. To explore whether capillary tube formation could be induced by geometric cues, we created different width (10- or 30-μm) linear adhesive islands that promoted cell–cell contact formation required for differentiation, yet differed in their ability to support cell spreading (Fig. 1). Cells on neighboring unpatterned regions of similar chemistry that supported unrestricted cell spreading were used as an internal control. When plated on these substrates, CE cells were found to spread most on the unpatterned substrates (mean projected cell area,

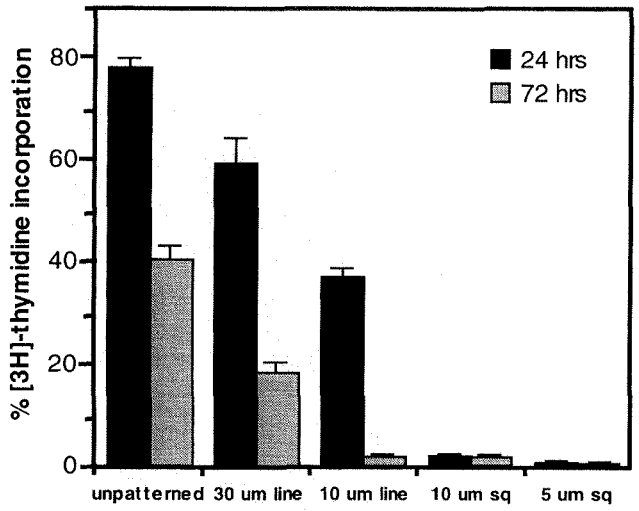

FIG. 2. Control of cell growth by cell area. The percentage of cells undergoing DNA synthesis at 24 and 72 h plotted as a function of the geometry of the ECM subtrate. S phase entry was measured by [^{3}H]thymidine autoradiography (200–300 nuclei were counted per point) in cells on 10- or 30-μm lines or 5 or 10-μm-wide squares. Cells on unpatterned regions exhibited the highest growth rate at all times. Cells on the 10-μm lines entered a nonproliferative phase by 72 h of culture. Studies were performed in triplicate.

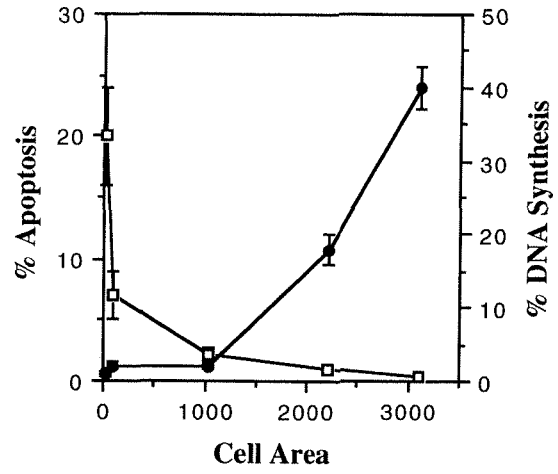

FIG. 3. Geometric control of CE growth and apoptosis. The projected cell area, measured at 24 h of culture, was directly proportional to the level of DNA synthesis (*solid circles*) and indirectly proportional to the level of apoptosis (*open squares*) in cells cultured on patterned substrates of different dimensions. Studies were performed in triplicate in CE cells plated on 5-μm-wide squares, 10-μm-wide squares, 10-μm lines, 30-μm lines, and unpatterned substrates.

3112 ± 300 μm^2), less on the 30-μm line (2200 ± 182 μm^2), and least on the 10-μm line (1042 ± 84 μm^2). The 10-μm line essentially allowed for only one or two cells to span its width whereas multiple cells could stretch across the wider 30-μm line.

Importantly, while cells initially proliferated when plated on all three adhesive substrates, the most highly spread cells (on unpatterned substrates) entered S phase at nearly twice the rate exhibited by the least spread cells (on 10-μm lines) during the first 24 h of culture (76 ± 2% versus 36 ± 3%). By 72 h in culture, the spreading-dependent effect on cell proliferation was magnified even further (Fig. 2). Cell proliferation rates remained high in spread cells but completely shut off in cells on 10-μm lines. Previous studies of CE cells cultured on square adhesive islands of different sizes ranging from 10 to 50 μm wide similarly showed that optimal growth (DNA synthesis) occurred in the most highly spread cells (mean projected cell area >2200 μm^2), whereas apoptosis was switched on in retracted cells with a mean projected cell area less than 500 μm^2 (2,3). However, the cells that spread on the 10 and 30-μm lines did not undergo apoptosis when analyzed with the TUNEL assay (Fig. 3). When the growth and apoptosis results from the present study were pooled with these previously published data (Fig. 2,3, Table 1), it became apparent that the projected area of cells on 10-μm lines (approximately 1000 μm^2) was too low to promote growth and too high to induce apoptosis. In contrast, the mean projected area of cells on the 30-μm line was approximately 2200 μm^2, a value that correctly predicted growth, although not at optimal levels.

The turning off of the growth and apoptosis programs observed in cells aligned on the 10-μm lines was accompanied by a concomitant switching on of the capillary differentiation program, as indicated by formation of linear cellular cords that appeared to possess a centralized hollow space (Fig. 4, Table 1). Formation of central lumina within these elongated cellular cords was confirmed by confocal microscopy with cells labeled with a fluorescent cytoplasmic dye (CMFDA). When cells plated for 72 h on 10-μm lines were visualized longitudinally by confocal microscopy, a single, continuous, central lumen could be seen to extend over several cell lengths along the main axis of the line (Fig. 4 *A,B*). When viewed in vertical cross-section (Fig. 4 *B*), a single CE cell body could be seen stretching around a negatively labeled lumen at its center. This tube-forming cell had partially retracted from the surface of the adhesive island such that only a small area of substrate adhesion was retained along its basal surface. The cells also appeared to increase in height such that other cytoskeletal systems (e.g., intermediate filaments) were no longer in a single focal plane characteristic of a spread cell in culture (not shown). In contrast, cells on the 30-μm lines always appeared as adherent, flattened monolayers when viewed by phase-contrast or confocal microscopy (Fig. 4 *A,C*). This alteration in adhesion did not appear to be due to a failure to realign since cells on both 10- and 30-μm lines oriented themselves lengthwise along the main long axis of the linear pattern within 48–72 h of plating, when visualized either by phase-contrast microscopy (Fig. 4 *A*) or by fluorescence microscopy after staining for F-actin with rhodaminated phalloidin (Fig. 5).

The development of strong CE cell–cell adhesions is critical for tube formation and PECAM is characteristic of these junctions

TABLE 1

SUMMARY OF DATA FOR BOVINE CAPILLARY ENDOTHELIAL CELLS CULTURED ON PATTERNED SUBSTRATES FOR 72 H[a]

Pattern	Cell area (μm^2)	DNA synthesis	Apoptosis	Lumen formation
10 μm sq	100	−	++	−
10-μm line	1042 +/− 84	−	−	++
30-μm line	2200 +/− 182	+	−	−
Unpatterned	3112 +/− 300	++	−	−

[a] A minus indicates no response; +, significant response ($P < 0.05$); ++, maximal response.

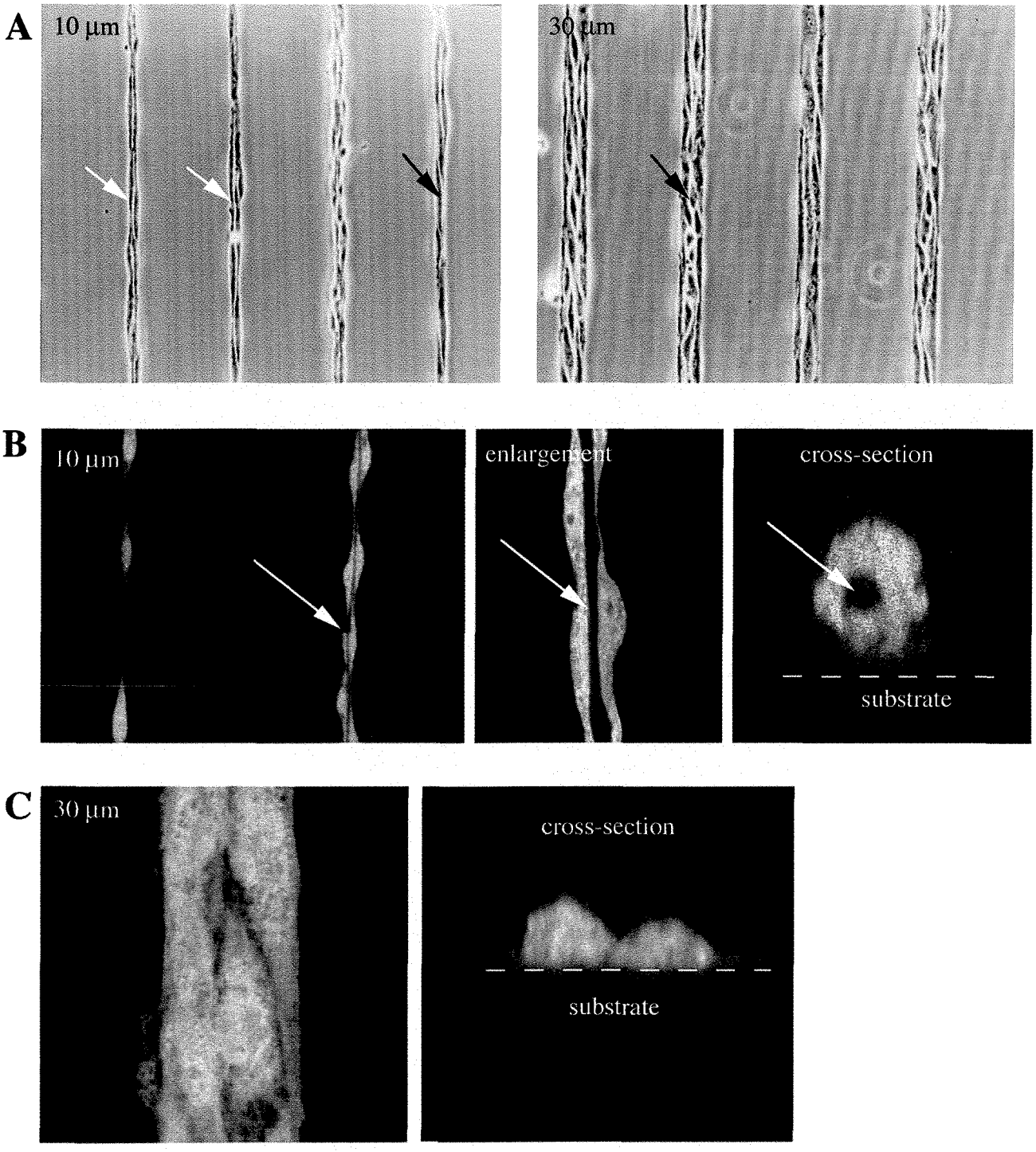

FIG. 4. Capillary tube formation by CE cells on linear patterns. *A*, Phase-contrast micrographs of CE cells cultured for 72 h on 10- or 30-μm lines. Magnification, ×200. Although cells aligned along the long axis of the lines on both substrates, only cells on the 10-μm lines formed tubes containing a central, phase lucent lumen (*white arrow*). *Black arrows* indicate multicellular cords that did not form tubes. *B*, Confocal microscopic images of CMFDA-stained cells cultured on 10-μm lines showed a central cavity extending along several cell lengths (*white arrow*) when viewed in a horizontal (XY) cross section (*left*; magnification, ×500). The lumenal cavity appears as a negatively stained central space when viewed at higher magnification in either XY (*middle*; magnification, ×1000) or vertical (XZ) cross sections (*right*; magnification, ×3000). *C*, Confocal microscopic images of cells cultured for 72 h on 30-μm lines showing that these cells remained spread within an adherent monolayer and did not form tubes. Magnification, ×1000.

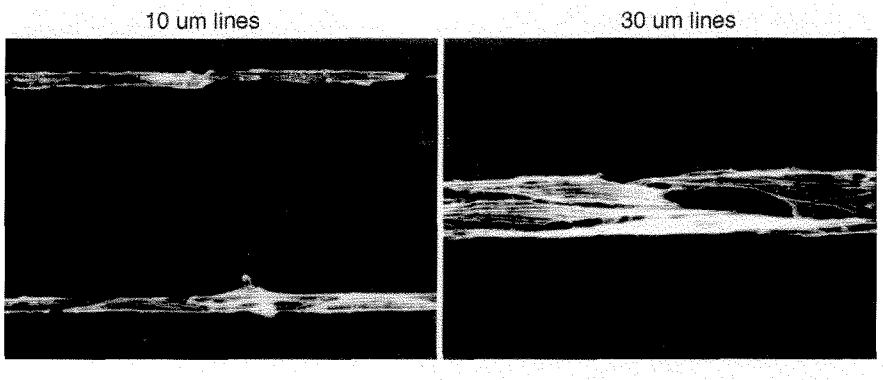

FIG. 5. Cytoskeletal alignment in cells cultured on 10- and 30-μm lines. Microfilaments (MF) aligned parallel to the main axis of the patterned substrate within 48–72 h in cells cultured on both 10- and 30-μm lines. Actin microfilaments were visualized by rhodamine-labeled phalloidin. Magnification, ×400.

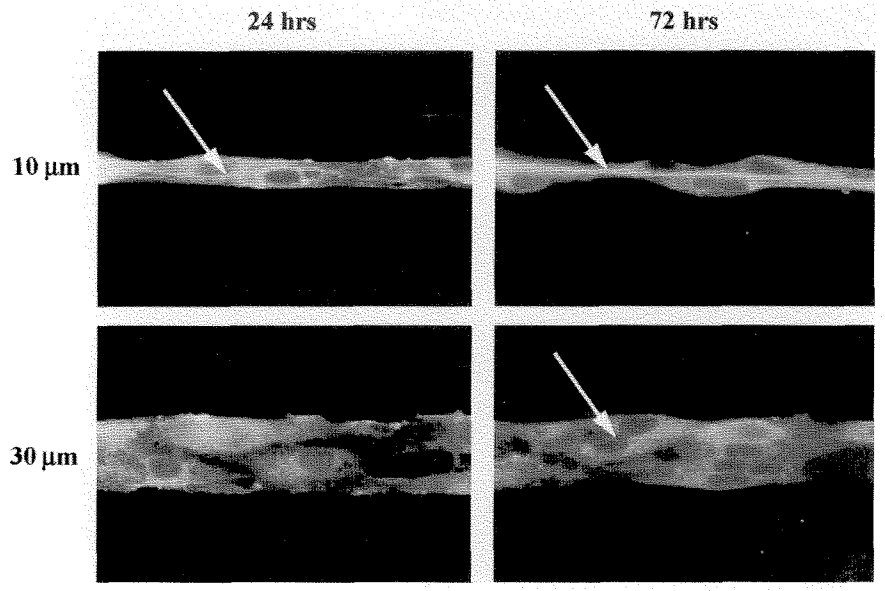

FIG. 6. Redistribution of the cell–cell adhesion molecule, PECAM, during tube formation. In cells cultured on 10-μm lines, PECAM initially was localized to discrete areas of cell–cell contact at 24 h (*white arrow*). By 72 h, PECAM appeared to form a continuous, linear junctional seal (*white arrow*). In cells cultured on 30-μm lines, PECAM staining was observed in local areas of cell–cell contact with increased time in culture (72 h; *white arrow*). A single continuous junctional seal, however, did not form. Magnification, ×630.

(8,34). At 72 h of cell attachment on 10-μm lines, linear cell–cell adhesions or junctional seals formed that extended along several cell lengths or at times, over the entire length of the tube, as indicated by continuous linear PECAM staining (Fig. 6). PECAM staining was also observed along the cell–cell borders in cells plated on 30-μm lines at 72 h of cell plating (Fig. 6). These patterns, however, were discontinuous suggesting that a complete linear junctional seal did not form in these cells.

Past studies have suggested that the mechanism of capillary differentiation involves complex interactions between CE cells and the ECM molecules they deposit (16). Immunofluorescence microscopy was used to explore the role of cell-derived ECM in the differentiation process by following changes in the distribution of FN and laminin (LM) in CE cells cultured on micropatterned lines over a 5-d period. We have previously shown that the distribution of FN staining is initially uniform across the adhesive island when the cell is first plated due to the preadsorption of FN on the substrate (2). Within 6–24 h after cell adhesion, FN remodeling began to be observed, as indicated by appearance of a fine, fibrillar pattern of FN beneath cells plated on both 10- and 30-μm lines (Fig. 7 *A*). Cells plated on the 30-μm line maintained this staining pattern over 5 d of culture. The staining pattern of FN in cells cultured on 10-μm lines, however, showed a dramatic reorganization within 48–72 h of plating. The FN fibers coalesced to form a single, large tendril as shown by immunofluorescence or confocal microscopy (Fig. 7 *A,B*). Cross-sectional views, as seen by confocal microscopy, revealed that the linear cord of FN extended underneath or between cells (Fig. 7 *C*). Similar results were obtained when antibodies against cell-derived LM were used (Fig. 8). After 4 d, cells cultured on the 10-μm lines pulled themselves off the rigid substrate as retracted tubular networks, while maintaining contacts with other cells and with the ECM tendrils.

DISCUSSION

ECM is known to play a key role in angiogenesis regulation, but the mechanism by which ECM exerts this effect remains unclear. Integrin receptor binding has been shown to stimulate chemical signaling events involved in this process (33,36). Other studies have suggested that mechanical determinants, such as cytoskeletal tension-dependent changes in cell shape, also play a role in switching between growth and differentiation during angiogenesis (13,15,16). Recent work with micropatterned surfaces demonstrated that cell shape—the degree to which a CE cell extends and flattens—is a key determinant of whether a cell enters the growth cycle or undergoes

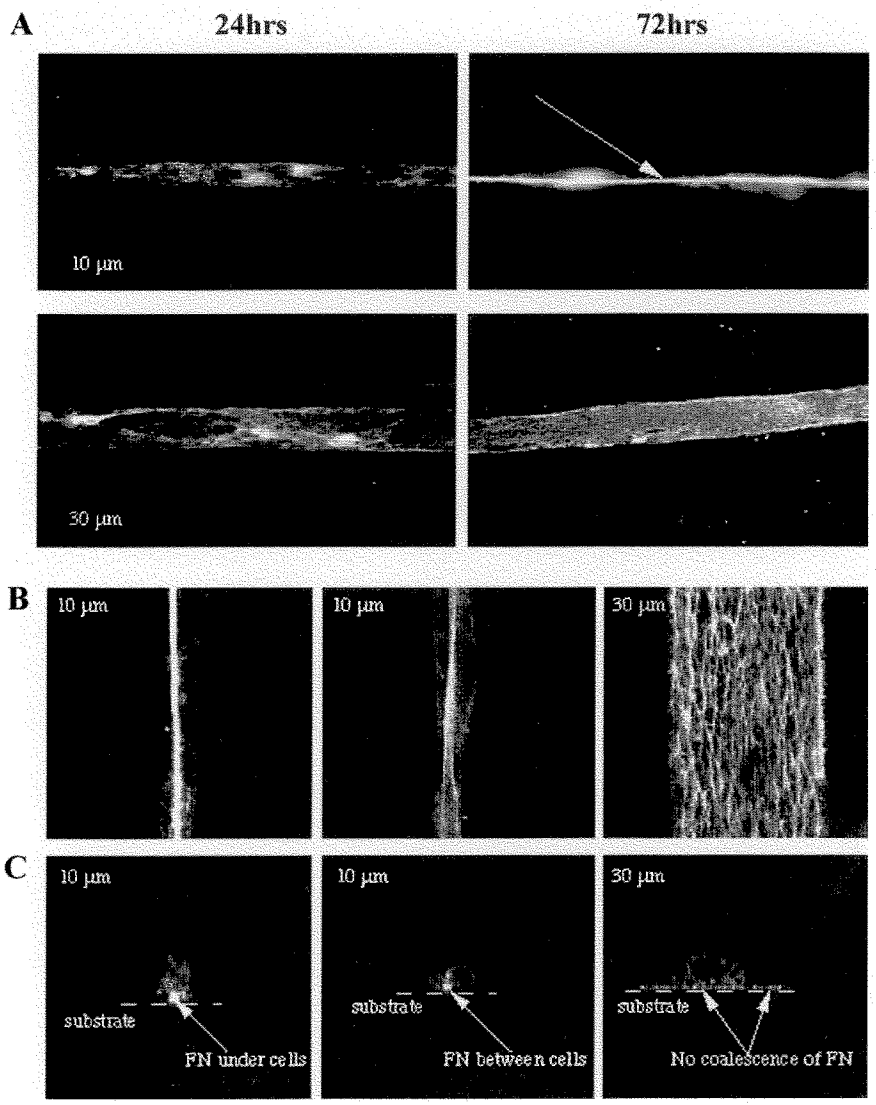

FIG. 7. Reorganization of FN by cells plated on 10-μm lines. *A*, Immunofluorescence micrographs showing FN staining in CE cells cultured on 10- and 30-μm lines for 24 and 72 h. FN appeared in a fibrillar pattern on both 10- and 30-μm lines after 24 h of culture. While similar FN staining was observed in cells on the 30-μm line after 72 h, FN reorganized to form a single linear thread within cells cultured on 10-μm lines. Magnification, ×630. *B*, Confocal micrographs showing horizontal (XY) cross sections in which FN reorganized into a central fibril within cells forming a tube on the 10-μm line but not in the cells growing as a monolayer on 30-μm lines. Magnification, ×1000. *C*, Confocal micrographs showing vertical (XZ) cross sections through CE cell cultures. *Note* that FN localized centrally in a single bright dot (thread in cross section) either underneath a single CE cell or between two cells on the 10-μm lines. In contrast, multiple smaller FN-containing dots appeared to be evenly distributed across the culture surface beneath cells cultured on 30-μm lines.

apoptosis (2,12). In the present study, we extended this analysis to show that the differentiation program which directs capillary tube formation also can be switched on geometrically. Patterns composed of lines 10 μm wide moderately restricted the extent of cell spreading such that neither growth nor apoptosis was induced. At the same time, the geometry of these lines promoted multicellular cell–cell interactions including the formation of PECAM-containing structures that extended to form linear junctional seals along the length of the developing tube. Simultaneously, linear ECM tendrils accumulated underneath and between the cells; this decreased the area of cell–substrate adhesion and promoted formation of continuous, hollow, tubular structures many cell diameters long. In contrast, cells plated on 30-μm lines formed cell–cell contacts but remained flattened on the culture substrate and did not differentiate into tubes. The micropatterned surfaces described here had identical chemistry; the substrates were coated with the same saturating density of FN, and the cells were cultured in the same FGF-containing medium. Thus, the culture of these cells differed only in a single parameter: a geometric difference of 20 μm in line width.

Substrate-immobilized FN promotes integrin clustering and the activation of associated integrin signaling pathways (e.g., Na^+/H^+ exchange, inositol lipid turnover) in CE cells (13,23,32). Small adhesive islands coated with a high density of FN that induce integrin clustering also activate early growth-signaling pathways (e.g., MAP kinase pathways), yet they do not support S phase entry (12). Larger islands that promote cell spreading, (i.e., greater than 1500 μm^2), induce both early signaling and later critical cell cycle events, such as upregulation of cyclin D1 and downregulation of the cdk inhibitor, $p27^{kip1}$ (12). Thus, while integrin ligation may stimulate early signaling events, the degree of cell spreading governs whether the cells will progress through the G_1/S restriction point and enter S phase. The present results show that if integrin signaling is activated and cell spreading is only promoted to a moderate degree, then CE cells are induced to enter a differentiation pathway. Specifically, cells on 10-μm-wide lines that restricted spreading to approximately 1000 μm^2 and promoted cell–cell contact formation turned on a tubular differentiation program. Cells on lines that differed in width by only 20 μm (30-μm lines), on the other hand, were more spread (2200

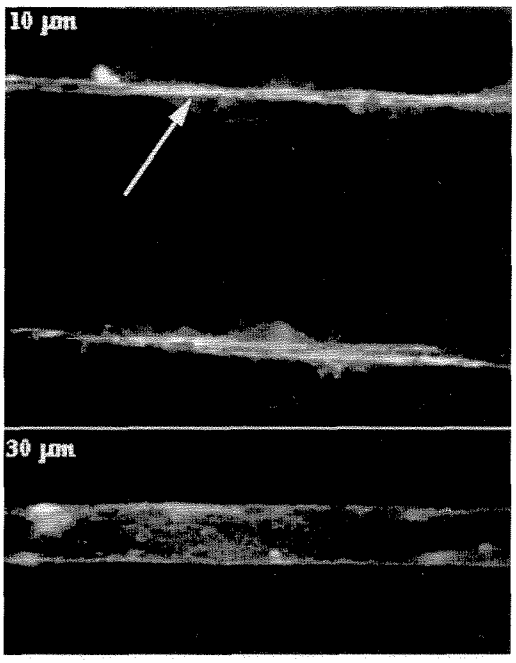

FIG. 8. Reorganization of laminin into a thread-like structure in cells cultured on 10-μm lines for 72 h. LM appeared in a threadlike staining pattern within the central core of the capillary tube after 72 h of culture on 10-μm lines. In contrast, a fine punctate pattern of LM staining was observed beneath cells on the 30-μm lines. Magnification, ×630.

μm^2), had higher levels of DNA synthesis, and failed to differentiate even though both cell–ECM and cell–cell adhesions formed normally. Our finding that cells on both linear substrates realigned their actin microfilaments was consistent with previous studies which suggested that microfilament alignment is responsible for cellular realignment and required for tube formation (5,7). However, our results demonstrate that while microfilament reorganization may be necessary for tube formation, it is not sufficient to commit cells to the differentiation pathway.

The endothelial-specific cell–cell adhesion molecule, PECAM, was observed at cell–cell junctions within 24–48 h in cells on 10-μm lines. Localization of PECAM to cell–cell junctions in cells on 30-μm lines occurred at 72 h, with cell confluence. As the cells on 10-μm lines developed into tubes, PECAM reorganized into a linear staining pattern suggestive of an interlocking zipper. Cell–cell adhesion molecules, such as PECAM, associate with the actin cytoskeleton (7,22). The alignment of the cytoskeleton and its associated PECAM-containing junctional complexes should significantly increase the net tensile stress that the cells with the multicellular cords can apply to their ECM adhesions. This would further enhance the alignment of ECM molecules and promote formation of thin linear ECM threads, as observed in this study. Over 72 h in culture, the cells apparently formed stronger attachments to the matrix fibril than to the original adhesive substrate so that cell-generated tractional forces promoted partial retraction of this tendril away from the surface of the adhesive substrate. A similar redistribution of the ECM was not observed in cells plated onto 30-μm lines, suggesting that the remodeling of the matrix into the thread-like configuration may be a key factor in tube development. These data also suggest that cellular and cytoskeletal realignment either precede the remodeling of the matrix or these events must happen simultaneously for tube formation to proceed.

These results are consistent with past studies on in vitro angiogenesis which demonstrated that tube formation involves multiple steps, including: 1) CE cell alignment and cellular cord formation, 2) accumulation of malleable ECM tendrils on the surfaces of adherent cells, 3) envelopment of the threads by the adherent cells, 4) exertion of cell-generated tension on these tendrils causing them to partially detach from the rigid substrate below, and 5) dissolution of the central ECM thread with concomitant accumulation of a new ECM along the abluminal surface and associated reversal of CE cell polarity to create a fully functional capillary tube (1,16,21). Furthermore, similar steps of capillary tube formation, including reversal of cell polarity, can be seen in vivo in the early blood islands of the developing embryo (6,30). Interestingly, CE cells underwent only the first four steps of this differentiation program in the present study; the central ECM tendrils never dissolved and the full differentiation program was not completed. This observation suggests that geometric cues are sufficient to switch CE cells out of growth or apoptosis and into a differentiation program. However, full completion of the tubular differentiation process may require additional signals, including other mechanical events. For example, in previous studies, dissolution of the central ECM tendril was preferentially promoted in regions in which the multicellular cords lost complete contact with the dish surface and were able to fully retract (16). This late step in tube formation, the dissolution of the central ECM, may have been inhibited in the present study because the multicellular cords maintained continuous contact with the rigid substrate along their length and thus did not retract (Fig. 4). In the few cases in which cord detachment was observed, the cords released completely from the substrate as a retracted tubular net and were not amenable to further analysis (data not shown).

Analysis of growth and apoptosis in cells cultured on linear patterns revealed that capillary differentiation occurs at a moderate degree of cell spreading that neither supports DNA synthesis nor programmed cell death (Table 1). This observation suggests that a common pathway may exist that regulates these three major gene cascades, rather than a model in which each program is independently regulated. Such a mechanism would ensure concomitant switching between different cell fates while preventing two programs from being initiated simultaneously. Our results demonstrate that this central mechanism of cellular control is regulated by changes in cell architecture. The mechanism by which cell shape regulates these genetic programs has yet to be elucidated. Previous studies, however, suggest that the integrity of the cytoskeleton and its ability to generate tension against a resisting substrate through integrin–ECM interactions may play an integral role in this control mechanism (2,12,14).

In summary, our results demonstrate the existence of a mechanical mechanism for switching CE cells between growth, differentiation, and apoptosis. In the presence of the same set of chemical signals (e.g., growth factors, integrin binding), different gene programs are activated depending on the degree of cell extension or retraction in the local microenvironment. While growth factors and integrin binding are necessary for the activation of all programs, cell geometry and the corresponding changes in the mechanical force balance within cells govern which genetic pathway is selected. These results are consistent with past studies that showed that the thickness and

malleability of the ECM change when CE cells switch between growth, differentiation, and death during angiogenesis in vivo (4,14,18,19). Development of a well-defined adhesive environment in which capillary tubes consistently form in vitro should facilitate future analysis of the complex, multistep process that mediates angiogenesis.

Acknowledgments

This work was supported by grants from NIH (HL57669 and GM30367), NSF (ECS972405), DARPA/SPAWAR/ONR. This work used MRSEC-shared facilities supported by the NSF (DMR-9400396). C. S. C. is grateful to the Angiogenesis Foundation for their generous support. J. T. thanks the NSF for a predoctoral fellowship.

References

1. Ausprunk, D. H.; Folkman, J. Migration and proliferation of endothelial cells in preformed and newly formed blood vessels during tumor angiogenesis. Microvasc. Res. 14:53–65; 1977.
2. Chen, C. S.; Mrksich, M.; Huang, S.; Whitesides, G. M., et al. Geometric control of cell life and death. Science (Wash DC) 276:1425–1428; 1997.
3. Chen, C. S.; Mrksich, M.; Huang, S.; Whitesides, G. M., et al. Micropatterned surfaces for control of cell shape, position and function. Biotechnol. Prog. 14:356–363; 1998.
4. Clark, E. R.; Clark, E. L. Microscopic observations on the growth of blood capillaries in the living mammal. Am. J. Anat. 64:251–301; 1938.
5. Cockerill, G. W.; Gamble, J. R.; Vadas, M. A. Angiogenesis: models and modulators. Int. Rev. Cytol. 159:113–147; 1995.
6. Coffin, J. D.; Poole, T. J. Embryonic vascular development: immunohistochemical identification of the origin and subsequent morphogenesis of the major vessel primordia in quail embryos. Development 102:735–748; 1988.
7. Cooper, J. A. Effects of cytochalasin and phalloidin on actin. J. Cell Biol. 105:1473–1481; 1987.
8. DeLisser, H. M.; Christofidou-Solomidou, M.; Strieter, R. M.; Burdick, M. D., et al. Involvement of endothelial PECAM-1/CD31 in angiogenesis. Am. J. Pathol. 151:671–677; 1997.
9. Dike, L. E.; Ingber, D. E. Integrin-dependent induction of early response genes in capillary endothelial cells. J. Cell Sci. 109:2855–2863; 1996.
10. Folkman, J. Tumor angiogenesis: therapeutic implications. N. Engl. J. Med. 285:1182; 1971.
11. Folkman, J.; Klagsburn, M. Angiogenic factors. Science. (Wash DC) 235:442–447; 1987.
12. Huang, S.; Chen, C. S.; Ingber, D. E. Control of cyclin D1, p27kip1 and cell cycle progression in human capillary endothelial cells by cell shape and cytoskeletal tension. Mol. Biol. Cell 9:3179–3193; 1998.
13. Ingber, D. E. Fibronectin controls capillary endothelial cell growth by modulating cell shape. Proc. Natl. Acad. Sci. USA 87:3579–3583; 1990.
14. Ingber, D. E.; Dike, L. E.; Hansen, L.; Karp, S., et al. Cellular tensegrity: exploring how mechanical changes in the cytoskeleton regulate cell growth, migration, and tissue pattern during morphogenesis. Int. Rev. Cytol. 150:173–220; 1994.
15. Ingber, D. E.; Folkman, J. How does extracellular matrix control capillary morphogenesis? Cell 58:803–805; 1989.
16. Ingber, D. E.; Folkman, J. Mechanochemical switching between growth and differentiation during fibroblast growth factor-stimulated angiogenesis in vitro: role of extracellular matrix. J. Cell Biol. 109:317–330; 1989.
17. Ingber, D. E.; Fujita, T.; Kishimoto, S.; Sudo, K., et al. Synthetic analogues of fumigillin that inhibit angiogenesis and suppress tumour growth. Nature (Lond) 348:555–557; 1990.
18. Ingber, D. E.; Jamieson, J. D. Cells as tensegrity structures: architectural regulation of histodifferentiation by physical forces transduced over basement membrane. In: Andersson, L. C.; Gahmberg, C. G.; Ekblom, P., ed. Gene expression during normal and malignant differentiation. Orlando: Academic Press, Inc.; 1985:13–32.
19. Ingber, D. E.; Madri, J. A.; Folkman, J. A possible mechanism for inhibition of angiogenesis by angiostatic steroids: induction of capillary basement membrane dissolution. Endocrinology 119:1768–1775; 1986.
20. Kudelka, A. P.; Verschraegen, C. F.; Loyer, E. Complete remission of metastatic cervical cancer with angiogenesis inhibitor TNP-470. N. Eng. J. Med. 338:991–992; 1998.
21. Kuzuya, M.; Kinsella, J. L. Reorganization of endothelial cord-like structures on basement membrane complex (Matrigel): involvement of transforming growth factor β1. J. Cell. Physiol. 161:267–276; 1994.
22. Matsumura, T.; Wolff, K.; Patzelbauer, P. Endothelial cell tube formation depends on cadherin 5 and CD31 interactions with filamentous actin. J. Immunol. 158:3408–3416; 1997.
23. McNamee, H. P.; Ingber, D. E.; Schwartz, M. A. Adhesion to fibronectin stimulates inositol lipid synthesis and enhances PDGF-induced inositol lipid breakdown. J. Cell Biol. 121:673–678; 1993.
24. Mrksich, M.; Chen, C. S.; Xia, Y.; Dike, L. E., et al. Controlling cell attachment on contoured surfaces with self-assembled monolayers of alkanethiolates on gold. Proc. Natl. Acad. Sci. USA 93:10775–10778; 1996.
25. Mrksich, M.; Dike, L. E.; Tien, J.; Ingber, D. E., et al. Using microcontact printing to pattern the attachment of mammalian cells to self-assembled monolayers of alkanethiolates on transparent films of gold and silver. Exp. Cell Res. 235:305–310; 1997.
26. O'Reilly, M. S.; Holmgren, L.; Chen, C.; Folkman, J. Angiostatin induces and sustains dormancy of human primary tumors in mice. Nat. Med. 2:689–692; 1996.
27. O'Reilly, M. S.; Holmgren, L.; Shing, Y.; Chen, C., et al. Angiostatin: a novel angiogenesis inhibitor that mediates the suppression of metastasis by a Lewis lung carcinoma. Cell 79:315–328; 1994.
28. Plopper, G. E.; McNamee, H. P.; Dike, L. E.; Bojanowski, C., et al. Convergence of integrin and growth factor receptor signaling pathways within the focal adhesion complex. Mol. Biol. Cell 6:1349–1365; 1995.
29. Prime, K. L.; Whitesides, G. M. Self-assembled organic monolayers: model systems for studying adsorption of proteins at surfaces. Science (Wash DC) 252:1164–1167; 1991.
30. Risau, W.; Flamme, I. Vasculogenesis. Annu. Rev. Cell Dev. Biol. 11:73–91; 1995.
31. Schwartz, M. A.; Ingber, D. E.; Lawrence, M.; Springer, T. A., et al. Multiple integrins share the ability to induce elevation of intracellular pH. Exp. Cell Res. 195:533–535; 1991.
32. Schwartz, M. A.; Lechene, C.; Ingber, D. E. Insoluble fibronectin activates the Na/H antiporter by clustering and immobilizing integrin alpha 5 beta 1, independent of cell shape. Proc. Natl. Acad. Sci. USA. 88:7849–7853; 1991.
33. Schwartz, M. A.; Schaller, M. D.; Ginsberg, M. H. Integrins: emerging paradigms of signal transduction. Annu. Rev. Cell Dev. Biol. 11:549–599; 1995.
34. Sheibani, N.; Newman, P. J.; Frazier, W. A. Thrombospondin-1, a natural inhibitor of angiogenesis, regulates platelet-endothelial cell adhesion molecule-1 expression and endothelial cell morphogenesis. Mol. Biol. Cell 8:1329–1341; 1997.
35. Singhvi, R.; Kumar, A.; Lopez, G. P.; Stephanopoulos, G. N., et al. Engineering cell shape and function. Science (Wash DC) 264:696–698; 1994.
36. Yamada, K. M. Integrin signaling. Matrix Biol. 16:137–141; 1997.